1 **Dual Function of Mitochondrial Complex III in *Plasmodium falciparum***

2 River S. Rell, Anurag Shukla, Joanne M. Morrisey, Ijeoma C. Okoye, Michael W. Mather, and

3 Akhil B. Vaidya

4 Center for Molecular Parasitology, Department of Microbiology and Immunology, Drexel

5 University College of Medicine, Philadelphia, PA 19129

6

Abstract

Complex III of the malaria parasite mitochondrial electron transport chain (mtETC) has been validated as an attractive target for currently used antimalarials. We previously showed that the main function of mtETC in blood stage *Plasmodium falciparum* is to regenerate ubiquinone, which serves as an obligatory co-substrate of dihydroorotate dehydrogenase (DHOD), an essential mitochondrial enzyme for pyrimidine biosynthesis. *P. falciparum* can be rendered resistant to all mtETC inhibitors by provision of a bypass mediated by cytosolic yeast DHOD, a fumarate-reducing enzyme. Malaria parasite mitochondrial DNA (mtDNA) encodes only 3 proteins, each a component of mtETC. However, attempts to eliminate mtDNA in transgenic parasites expressing yDHOD have been unsuccessful, suggesting the possibility that essential function(s) other than the canonical redox reactions of the mtETC also require mtDNA maintenance. Here we have tested the hypothesis that Complex III serves the dual functions of processing imported mitochondrial proteins, as well as ubiquinone regeneration. We have generated transgenic lines that conditionally express mitochondrial processing peptidase a (MPPα), which is also a component of Complex III. Using these parasites, we have determined that MPPα is essential even when the need for mitochondrial electron transport is bypassed. MPPα knockdown also resulted in hypersensitivity of the parasites to proguanil, a drug that synergizes with mtETC inhibitors such as atovaquone. Pulldown with MPPα followed by proteomics revealed the association of multiple mitochondrially targeted proteins, in addition to all components of Complex III. These results are consistent with the suggestion that Complex III in *P. falciparum* serves both mtETC and protein processing functions in mitochondrial physiology.

30 **Introduction**

31

32 Mitochondrial Complex III in Apicomplexan parasites is a clinically validated drug target,
33 and inhibitors of it are in therapeutic use. Divergence of the parasite Complex III from the host
34 underlies the selectivity of these potent drugs (1, 2). Working through a modified Q cycle (3, 4),
35 Complex III catalyzes the transfer of electrons from ubiquinol to cytochrome *c* while
36 transporting protons into the mitochondrial intermembrane space. Inhibition of this step in
37 mtETC results in blockage of all mitochondrial dehydrogenases that require ubiquinone as the
38 electron acceptor. In previous studies, we have shown that in the blood stage *P. falciparum* the
39 only critical dehydrogenase for parasite survival is dihydroorotate dehydrogenase (DHOD), an
40 essential enzyme that is required for pyrimidine biosynthesis by the parasites (5). When the
41 parasites are genetically modified to express cytosolic yeast DHOD (yDHOD), they are rendered
42 independent of mtETC, since yDHOD uses fumarate as the electron acceptor, rather than
43 ubiquinone (5). This metabolic bypass rendered the parasites resistant to all mtETC inhibitors
44 such as atovaquone. Mitochondrial DNA (mtDNA) in malaria parasites is highly reduced in size
45 and encodes only three proteins, each a component of mtETC (cytochrome *b* and subunits I and
46 III of cytochrome c oxidase) (1, 6, 7). Therefore, we reasoned that it should be possible to
47 eliminate mtDNA from mtETC-independent parasites expressing yDHOD. However, our multiple
48 attempts to achieve this by disrupting genes encoding mitochondrial functions required for
49 mtDNA maintenance and mitochondrial translation have failed in transgenic parasites
50 expressing yDHOD (8-10). Thus, it is likely that the mtETC complexes serve one or more
51 functions in addition to respiration in blood stage malaria parasites. At present the nature of
52 these functions remains unknown.

53 Except for the 3 proteins encoded by the parasite mtDNA, all mitochondrial proteins are
54 encoded in the nuclear genome, translated in the cytoplasm and imported into the
55 mitochondrion. Many of these proteins contain targeting peptides at their N-termini. These
56 peptides are cleaved off by mitochondrial processing peptidase (MPP) (11, 12). MPPs in
57 mammalian and yeast mitochondria consist of heterodimers of α and β subunits that are
58 localized within the mitochondrial matrix (13, 14). The catalytic sites are present within the β
59 subunit, which is a metalloprotease with a Zn^{2+} ion at the active site (15). The α subunit does
60 not have catalytic property but is essential for substrate recognition and proper presentation of
61 the peptide within the catalytic site in multiple steps (16, 17). In addition to the matrix-localized
62 MPP in fungi and mammals, Complex III in eukaryotes also contain Core1 and Core2 subunits
63 that have high sequence homology to the MPP subunits α and B, respectively (17-19). These
64 subunits in yeast have lost their catalytic activity, whereas in mammals they serve to process
65 just one protein, the Rieske 2Fe2S subunit of Complex III (20, 21). Hence, the majority of
66 mitochondrial proteins in these organisms have to be processed by the matrix located MPP. In
67 stark contrast, plant mitochondria do not contain matrix located MPPs, which led Braun to
68 suggest that Complex III associated Core proteins fulfilled MPP function, as later confirmed, and
69 thus Complex III has dual functions in plants: ubiquinol oxidation to serve mtETC and processing
70 of mitochondrially targeted proteins (22, 23). We hypothesize that in malaria parasites correct
71 assembly of Complex III is essential not just for its function in mtETC but also for processing
72 most imported mitochondrial proteins. Thus, even when mtETC has been rendered redundant,
73 Complex III would still need to be assembled to process mitochondrial proteins. In this study we

74 have used conditional expression of MPPα to investigate the potential dual role of Complex III
75 in blood stage *P. falciparum*.
76
77
78 **Materials and Methods**

79 ***P. falciparum* culture and transfection**
80 We used *P. falciparum* D10_VP2KO, in which the pfVP2 locus encoding a type 2 H^+ pumping
81 pyrophosphatase was disrupted with the yDHOD selectable maker, for transfections (24). These
82 parasites are resistant to all mtETC inhibitors, as well as inhibitors of parasite DHOD.
83 *D10_VP2KO and Dd2attb* asexual blood stage parasites were cultured in human (O+) RBC, at
84 2.5% hematocrit in RPMI1640 medium supplemented with 0.5% Albumax, 2 g/liter $NaHCO_3$, 15
85 mM HEPES pH 7.4 , 1 mM hypoxanthine and 50 mg/liter gentamicin in 90% N_2, 5% O_2 and 5%
86 CO_2. Testing for Mycoplasma was done on a regular basis to ensure the cultures were free of
87 any such infection.

88 For transfection, parasite cultures with 5-7% ring stage parasites were washed three
89 times with Cytomix. The parasites were resuspended to 50% hematocrit in Cytomix. 50 µg of
90 linearized pMG75 MPPα plasmid isolated using a Qiagen Maxikit (Qiagen, Valencia, CA, USA)
91 and precipitated in ethanol was centrifuged down and resuspended in 100 µl Cytomix. The
92 plasmid and 250 µl of the parasite cytomix suspension were combined and transferred to a 0.2
93 cm electroporation cuvette on ice. Electroporations were carried out using a BioRad GenePulser
94 set at 0.31kV, 960uF. The electroporated cells were immediately transferred to a T-25 flask

95 containing 0.2 ml uninfected 50% RBCs and 10 ml medium. Parasites were selected using 2.5
96 µg/ml Blasticidin and 250 nM anhydrotetracycline (aTc).

97 **Transfection vector generation**

98 Optimal gRNA sequences were identified using CRISPOR software to generate a double strand
99 break within the endogenous MPPα locus (25). gRNA sequences were cloned into a Cas9-sgRNA
100 vector (26)(S1A and B).

101 pMG75 (27) plasmid backbone was used to construct the repair template vector used to help
102 generate D10_VP2KO_MPPα, the MPPα conditional knockdown line in the D10_VP2KO
103 background. (24). A synthetic gene block was ordered from GenScript containing 584 base pair
104 MPPα 5' homologous region (nucleotide 1591-2175) in the coding sequence, containing silent
105 blocking mutations in the selected gRNA recognition site, and 550 base pair 3'homologous
106 region (nucleotide 2178-2728) in the 3'UTR, separated by a linker region containing restriction
107 enzyme sites for SacII and BspEII for linearization of the plasmid. The homologous regions are
108 flanked by BstEII and BssHII for ligation into the pMG75 backbone, which contains the TetR-
109 DOZI-aptamer regulatory system, as well as a BSD selectable marker. The synthetic gene was
110 inserted into the pMG75 plasmid backbone via T4 DNA ligase. All plasmids were sequenced
111 using Plasmidsaurus (South San Francisco) nanopore sequencing. The plasmid was linearized
112 with SacII and BspEII before transfection.

113

114 **Growth Assay**

115 Parasites were enriched for late trophozoite and early schizont stages using a layered step
116 gradient of 70%, 60%, and 35% Percoll. Equal amounts of synchronized parasites were split into
117 a 6 well plate containing Human (O+) RBC at 2.5% hematocrit in 10ml of complete RPMI
118 medium. Triplicate cultures were grown in the presence or absence of aTc, with daily medium
119 change. Cumulative parasitemias were counted over the span of 8 days using flow cytometry
120 after staining with SYBR Green. Cumulative parasitemias were plotted using GraphPad Prism.

121 **Immunofluorescence assays.**

122 50 µL of packed volume parasite cultures were fixed with 4% v/v paraformaldehyde and
123 0.0075% v/v glutaraldehyde with slow mixing in a rotor for one hour at room temperature. The
124 cells were washed 3x with PBS, followed by permeabilization with 0.125% v/v Triton X-100 in
125 PBS. The cells were treated with $NaBH_4$ (0.1 mg/ml) for five minutes at room temperature while
126 mixing on a rotor. Samples were washed twice with 1X PBS and then blocked with 3% w/v BSA
127 for 1 hour. Anti-HA (Lot#12923, Santa Cruz Biotechnology) and anti HSP60 (Lot# PP487392
128 Novus Bio) antibodies were added to the parasites at 1:500 dilution, and the samples were
129 incubated overnight at 4°C in a rotor. Following three PBS washes, Alexa Fluor 488 conjugated
130 goat anti-mouse IgG (Invitrogen Lot# SG251135) and Alexa Flour 568 conjugated goat anti-
131 rabbit (Invitrogen lot #2447870) secondary antibodies were added at 1:250 dilution, followed
132 by overnight incubation at 4°C. After three PBS washes, the treated parasite samples were
133 resuspended in anti-fade buffer (S2828, ThermoFisher Scientific) and imaged using a Nikon Ti
134 microscope.

135 **Live Cell Microscopy**

136 35 mm glass bottom culture dishes were coated with 0.1% poly-D-lysine overnight and washed
137 3 times with PBS. 250 µL of 2.5% hematocrit parasite culture was added to the dishes and
138 incubated for 30 min to allow attachment. Culture dishes were washed 3 times with 1XPBS
139 followed by addition of phenol red-free RPMI. Parasites were stained with 62.5 nM
140 MitoTracker Red (Life Technologies by ThermoFisher Scientific) for 20 minutes, followed by 0.5
141 mg/ml Hoechst nuclear staining for 10min. Imaging was done using the Nikon Ti microscope.
142 Parasites were temperature controlled at 37 °C. Hoechst-stained parasites were visualized with
143 the DAPI filter set, while MitoTracker red was visualized using the tetramethyl rhodamine
144 isocyanate (TRITC) filter set. Images were 2-dimentionally deconvoluted and processed using
145 Nikon NIS Elements (5.30.02) Imaging Software. The presence of mitochondrial membrane
146 potential or parasite plasma membrane potential was visualized following incubation with
147 MitoTracker red. For statistical analysis of the membrane potential visualization, 30 parasites
148 were counted and imaged. The results were graphed using GraphPad Prism.

149 **Western blotting**

150 Saponin lysed parasite pellets were suspended in approximately ten volumes of 2% w/v SDS,
151 5% β-mercaptoethanol, and 1% bromophenol blue. Samples were centrifuged for 5 minutes at
152 13,000g, and the supernatant was subjected to SDS-PAGE. The separated proteins on the gel
153 were transferred to PVDM membranes at 20 volts overnight. Powdered milk solution was used
154 to block the membranes. Blots were then incubated at a dilution ratio of 1:10,000 with primary
155 antibody. After probing with primary antibody (Mouse monoclonal anti-HA Lot#12923, Santa

156 Cruz Biotechnology, Rabbit anti- *Plasmodium* aldolase Lot#GR289448-4 ABCAM, Rabbit anti
157 HSP60 Lot# PP487392 Novus Bio) blots were washed with Tris-buffered saline with tween
158 (TBST) and incubated with secondary antibody (Goat anti mouse IgG-HRP Lot#GR3219575-4
159 ABCAM, Mouse anti rabbit IgG-HRP Lot#L1819 Santa Cruz Biotechnology) conjugated with
160 horseradish peroxidase at a concentration of 1:10,000.

161 **Immunopulldown and Proteomics**

162 100 µL parasite pellets from both wildtype and D10_VP2KO_MPPα were solubilized overnight
163 at 4°C in solubilization buffer containing 2% digitonin, 200 mM 6- aminocaproic acid, 50 mM
164 Bis-tris, pH 7, 1 mM EDTA, 1 mM AEBSF, and protease inhibitor cocktail (Sigma-Aldrich). The
165 solubilized sample was centrifuged at 14,000 rpm for 15 min at 4 °C to remove debris, and the
166 supernatant was incubated with anti HA antibody coated magnetic Dynabeads (Pierce Anti-HA,
167 Clone 2-2.2.14, Clone 9E10; Thermo Fisher Scientific). Beads were washed 3 times in 1x PBS,
168 and solubilized total protein was added to 50 µl of the beads, followed by overnight mixing by
169 rotation at 4 °C. Protein-bound beads were washed three times with 1x PBS + 0.02% digitonin.
170 Beads with bound proteins were used for LC/MS on bead proteomics at the University of South
171 Florida Mass Spectrometry & Proteomic Core Facility. Protein samples were prepared for LC-
172 MS/MS using S-Traps (Protifi). 5% SDS in 50 mM triethylammonium bicarbonate (TEAB) was
173 added to the IP beads. Protein samples were reduced with 20 mM dithiothreitol (DTT) at 95 °C
174 for 10 min and alkylated using 40 mM iodoacetamide (IAA) in the dark at room temperature for
175 30 min. The samples were acidified with 12% phosphoric acid (final concentration 1.2%) before
176 adding 6x volumes of S-trap buffer (90% Methanol, 100 mM TEAB). The protein solution was

177 loaded onto micro S-traps, and centrifuged at 4000xg for 30 sec. Three washes with 150 µl S-
178 trap buffer were performed. 0.5 µg of Trypsin/LysC (Promega) was added to the S-trap filter
179 and digested overnight (~16 hrs) at 37 °C. Peptides were eluted with sequential additions of 50
180 mM TEAB, water+0.1% formic acid, and 50/50 acetonitrile/water+0.1% formic acid, centrifuged
181 at 4000xg for 1 min each. Peptides were completely dried in a vacuum-centrifuge concentrator
182 before resuspension in water+0.1% formic acid.

183 Peptides were separated using a Vanquish Neo UHPLC (Thermo) with a 50 cm EASY-Spray
184 PepMap Neo C18 column (Thermo) and analyzed on a Q Exactive Plus hybrid quadrupole mass
185 spectrometer (Thermo). Peptides were separated over a 1hr gradient (Mobile Phase A:
186 water+0.1% Formic Acid, Mobile Phase B: Acetonitrile+0.1% Formic Acid; 2% B-32% B), and data
187 was acquired using data-dependent acquisition (DDA) with a Top 30 method. Full MS scans
188 were acquired at 70k resolution, MS/MS scans were acquired at 17.5k resolution. Raw data files
189 were searched using MaxQuant (v2.4.9) against the current *Plasmodium falciparum* proteome
190 sequences downloaded from PlasmoDB.org, as well as MaxQuant generated databases of
191 reverse protein sequences and common contaminant protein sequences. Digestion settings
192 specified Trypsin/P specific enzyme digestion, with a maximum of 2 missed cleavages and a
193 minimum peptide length of 7. Both PSM (peptide spectral match) and protein FDR cutoffs were
194 set at 1%. Cysteine carbamidomethylation was set as a fixed modification. Methionine
195 oxidation and acetylation (protein N-term) were set as variable modifications. The MS/MS
196 match mass tolerance was set at 20ppm. Label Free Quantification intensities of enriched
197 proteins were compared across the replicates to determine fold change and statistical
198 significance using pair wise Student t-test. Volcano plots were visualized using Graphpad Prism.

199 **Growth inhibition assay**

200 All parasite growth inhibition assays were performed in triplicate in 96-well plates as described
201 by Desjardin et al. (28). *P. falciparum*-infected erythrocytes had aTc removed 48 hours prior to
202 the start of the assay. At 1.0% initial parasitemia and 1.5% hematocrit, these parasites were
203 exposed to various concentrations of the indicated drug/inhibitor for 48h and then pulsed with
204 0.5 µCi of ^{3}H-hypoxanthine for an additional 24h. Untreated parasitized and unparasitized red
205 blood cells were incubated concurrently with the treated parasites as controls for growth and
206 radioactive precursor incorporation. The 96 well plates were then frozen at -80°C for 24 h to
207 disrupt erythrocyte and parasite membrane integrity. Following freezing, the plates were
208 warmed to 37°C, and parasites were harvested onto EasyTab™-C Self-Aligning Glass Fiber Filters
209 (Packard, Meridian, CT, USA). The filters were then dried completely and placed into an
210 Omnifilter™ 96-well plate filter case (Packard, Meridian, CT, USA). 30µl of OmniScint™ (Packard,
211 Meridian, CT, USA) scintillation fluid was added to each well and the radiation was counted with
212 a TopCount™ counter. The incorporation of radioactivity into nucleic acids served as a measure
213 of cell proliferation and is reported by TopCount as counts per minute (cpm). The total cpm of
214 the non-parasitized red blood cells was subtracted from the cpm of all other wells. The cpm of
215 each sample was converted to percent by dividing it by the cpm of the untreated control. The
216 percent growth versus drug/inhibitor concentration was plotted using GraphPad Prism software.
217 A nonlinear regression dose-response curve was calculated in Prism after adjusting the lowest
218 percent to equal zero and the highest percent to 100.

219

220 **Results**

221 **Generation of parasite lines conditionally expressing MPPα**

222 A parasite line expressing yDHOD (D10_VP2KO) was chosen as the parental line to
223 prepare the MPPα conditional knockdown line. These parasites are independent of mtETC
224 activity and are resistant to all mtETC inhibitors (5, 29). We modified the endogenous MPPα
225 locus (PF3D7_0523100) in D10_VP2KO parasites using CRISPR-Cas9 to generate parasites
226 conditionally expressing 3HA-tagged MPPα under regulation of the aptamer-TetR-DOZI system
227 (Figure S1). PCR confirmed the integration of the expected portion of the donor plasmid within
228 the modified MPPα locus (Figure 1A and B). Localization of MPPα -3HA was determined by
229 immunofluorescence using anti-HA antibody (Figure 1C). We used HSP-60 antibody as a
230 mitochondrial marker to demonstrate colocalization of MPPα at the parasite mitochondrion, as
231 shown in Fig. 1C.

232 **Figure 1: Generation of parasite lines conditionally expressing MPPα** (A) Schematic of MPPα
233 locus modification using CRISPR-Cas9. Vertical arrow indicates position of sgRNA binding. Also
234 indicated are the 5' and 3' homologous regions (HR), 5' HR coming from MPPα CDS and the 3'
235 HR coming from 3'UTR. (B) Using primers indicated by PCR1, amplification of the forward and
236 reverse primers from the endogenous locus shows that the locus is disrupted in the MPPα
237 transfected line. Using primers indicated for PCR2, amplification of the forward primer from the
238 endogenous locus and the reverse primer from the HA tag present in the plasmid determines
239 correct integration of the donor DNA into the parasite genome. (C) Representative
240 immunofluorescence images of a parasite conditionally expressing MPPα, showing its
241 mitochondrial localization.

242 **MPPα is essential for parasite viability**

243 We assessed expression of MPPα in the presence and absence of aTc by carrying out
244 western blot analysis of parasite lysates collected over 8 days of parasite cultures; HSP60

245 expression was used as a loading control. As shown in Fig. 2A and B, expression of MPPα was
246 below detection level by day 4 of parasite growth in absence of aTc. We assessed the effects of
247 MPPα knockdown on parasite growth by removing aTc at the trophozoite stage of the parasite.
248 As shown in Fig. 2C, parasite growth ceased in the second cycle following aTc removal. No
249 viable parasites were detected via Giemsa stain in MPPα (-) condition by day 6 following aTc
250 removal. Since these studies were carried out using a parasite line that was independent of
251 mtETC activity by having the metabolic bypass provided by yDHOD, suggesting that MPPα
252 serves a critical function in addition to supporting mtETC activity as a subunit of complex III.

253

254 **Figure 2: MPPα is essential for parasite viability.** (A) Western blot analysis using anti-HA
255 and anti-HSP60 antibodies. (B) Quantification of Western blot normalized to intensities of anti-
256 HSP60. Pixel intensities were measured via Image J. (C) Assessment of growth of MPPα (+) and
257 MPPα(-) parasites. Growth assay data was conducted in triplicate by flow cytometry using SYBR
258 green stained parasites.

259

260 **Mitochondrial membrane potential is disrupted in knockdown parasites.**

261 Maintenance of electrochemical potential across the inner mitochondrial membrane is
262 critical for the survival of all eukaryotes. We have previously shown that blood stages of
263 *Plasmodium falciparum* have two independent means to maintain mitochondrial membrane
264 potential: one dependent on mtETC and the other independent of mtETC (5). Therefore, we
265 next examined mitochondrial membrane potential in parasites with and without MPPα
266 expression. Using live cell microscopy, the presence of mitochondrial membrane potential was
267 visualized using Mitotracker red staining in both knockdown and wild type parasites. After one

268 cycle of MPPα knockdown, 40% of the parasites were observed to have a diffused Mitotracker
269 staining, which is indicative of collapsed mitochondrial membrane potential. Since parasite
270 plasma membrane potential remains intact (initially), the positively charged probe accumulates
271 within the cytoplasm, but dissipation of the mitochondrial membrane potential would prevent
272 its accumulation in the mitochondrion. After two cycles, 73% of knockdown parasites displayed
273 diffuse staining. By Day 6 of MPPα knockdown, no parasites with mitochondrial staining were
274 visible (Figure 3A and B). While MPPα depletion may directly affect mtETC, the secondary
275 pathway for mitochondrial membrane potential should remain operative. Thus, these data
276 indicate that removal of MPPα affects both the primary and secondary pathways for generating
277 membrane potential.
278
279
280 **Figure 3: Mitochondrial membrane potential is disrupted in knockdown parasites.** (A)
281 Live cell microscopy images of MPPα (+) and MPPα (–) parasites. Mitotracker staining (red)
282 revealed tubular morphology in MPPα(+) parasites but was diffused in varying number of
283 MPPα(-) parasites starting as early as Day 2 following the knockdown (B) Quantitation of
284 morphological profiles of 30 parasites at each time points was assessed, showing gradual
285 increase in parasites showing diffuse Mitotracker staining resulting from disruption of
286 mitochondrial membrane potential.

287 **Knockdown of MPPα expression causes hypersensitivity to proguanil.**

288 A commonly used antimalarial drug, Malarone, is a synergistic combination of atovaquone and
289 proguanil (30, 31). We have previously shown that the synergistic property of proguanil results
290 from its inhibition of the secondary pathway for mitochondrial membrane potential generation
291 (5). Since MPPα depletion affects both mtETC dependent and independent pathways of
292 generating membrane potential (Figure 4A), we wanted to investigate whether the absence of

293 MPPα influences proguanil sensitivity of the parasites. We carried out growth inhibition assays
294 using ^{3}H-hypoxanthine incorporation by parasites treated with proguanil in presence and
295 absence of MPPα. While MPPα(+) parasites showed EC50 of 1585 nM for proguanil, MPPα(-)
296 parasites were approximately 200-fold hypersensitive to proguanil with EC50 of 8.4 nM (Figure
297 4B). In contrast, there were no changes in response of the parasites to other inhibitors (DSM1,
298 atovaquone and PA21A092) in presence or absence of MPPα (Figure S3). We have previously
299 shown that ubiquinone analogue, decyl-ubiquinone, is able to partially rescue parasite growth
300 when subjected to Complex III inhibition (32). Thus, we assessed the ability of decyl-
301 ubiquinone to reverse hypersensitivity to proguanil in MPPα(-) parasites. Addition of 25 μM
302 decyl-ubiquinone had only a relatively minor effect on hypersensitivity to proguanil in MPPα(-)
303 parasites (Figure 4C).

304

305 **Figure 4: Knockdown of MPPα expression causes hypersensitivity to proguanil.** (A) Parasite
306 growth inhibition assessed by ^{3}H-hypoxanthine incorporation following proguanil treatment.
307 For MPPα- parasites, aTc was removed for 48 h followed by ^{3}H-hypoxanthine addition for 72hr.
308 MPPα(+) parasites were also grown for 72hr followed by ^{3}H-hypoxanthine addition. (B) EC_{50}
309 values for DSM1, atovaquone, PA21A092, and proguanil in MPPα+ and MPPα- parasites. While
310 the EC50 values for Complex III, DHOD and PfATP4 inhibitors were similar for MPPα(+) and
311 MPPα(-) parasites, MPPα(-) parasites were almost 200-fold hypersensitive to proguanil. (C)
312 Parasite growth inhibition assessed by ^{3}H-hypoxanthine incorporation following proguanil
313 treatment and addition of 25 μM decyl-ubiquinone where indicated. For MPPα(-) parasites, aTc
314 was removed for 48 h followed by ^{3}H-hypoxanthine addition for 72hr.

315 **Proteomic analysis of MPPα immunoprecipitation**

316 To gain insight into interactions of MPPα with other mitochondrial proteins, we carried
317 out immunoprecipitation from both MPPα tagged and wildtype parasites using anti-HA beads

318 followed by LC-MS/MS analysis. Overall, 93 proteins were identified as significantly enriched in
319 the MPPα immunoprecipitated protein samples, using a cutoff of two-fold change compared to
320 the control with p-value <0.05 (Figure 5A). Of the putative 12 subunits of Complex III, 11
321 subunits, including mitochondrially encoded cytochrome *b,* were enriched greater than a
322 million-fold, based on the label free quantification (LFQ) intensity of the peptides observed.
323 QCR13 (Pf3D7_0817800) was the only putative Complex III protein that was absent, likely due
324 to its small size of just 54 amino acids. Remarkably, there were 45 additional predicted or
325 experimentally confirmed mitochondrial proteins that were equally significantly enriched. This
326 suggests their interactions with MPPα are of similar magnitude as MPPα's association with
327 Complex III. We postulate the presence of these mitochondrial proteins with MPPα being by
328 virtue of their transient association during processing of their mitochondrial targeting peptides.
329 The significance of additional proteins that were enriched but not predicted to be
330 mitochondrial remains unclear. It is interesting to note, that cytochrome *c* oxidases subunits 1
331 and 3 were not enriched. This is likely due to these proteins being encoded by mtDNA and not
332 requiring processing of mitochondrial targeting sequences (1,6) . These data suggest that
333 Complex III is engaged in the dual functions of mtETC integrity, as well as processing imported
334 mitochondrial proteins.

335

336 **Figure 5: Proteomic analysis of MPPα immunoprecipitation** (A) Volcano plot of
337 enriched proteins with a $\log_2$-fold change of label free quantification (LFQ) intensity and p-
338 values of < 0.05 found in immunoprecipitated MPPα samples. The red dots represent proteins
339 present in Complex III. The purple dots represent proteins that are predicted to be targeted to
340 the mitochondria. The blue dots represent the other proteins that were significantly enriched in

341 the immunoprecipitated samples. (B) Pie chart depicting the number of proteins that fall into
342 the categories of Complex III, likely mitochondrially targeted, and other enriched proteins.

343 **Discussion**

344 Although mitochondria in all extant organisms originated from the symbiotic
345 arrangement between an archaeon and an α-proteobacterium that led to the emergence of
346 eukaryotes, mitochondrial genomes and physiology are as divergent as the organisms in which
347 they reside (33, 34). Oxidative phosphorylation to generate ATP, while a major function of
348 mitochondria in many organisms, is not essential in some organisms, especially those that live
349 in anaerobic environments (35). Indeed, such organisms often lack mtDNA but continue to
350 possess a remnant mitochondrion called a mitosome (36, 37). In addition, certain yeasts (38),
351 cultured vertebrate cells (39) and bloodstream-forms of trypanosomes (40) can be manipulated
352 to lose their mtDNA while maintaining the mitochondrion itself. These are called rho^0 cells, and
353 investigations with such rho^0 cells have helped to establish that the absolute essential function
354 of their retained mtDNA-negative mitochondria is to synthesize and export inorganic Fe-S
355 clusters for a variety of iron-sulfur proteins required for cell survival (41, 42). To permit this
356 essential function, mitochondria need to maintain an electropotential across their inner
357 membrane, which is required for protein and metabolite transport. In mitochondria with an
358 active mtETC the membrane potential is normally established through proton pumping by the
359 respiratory complexes. A lack of mtDNA will lead to the absence of mtETC, so then the
360 electropotential will need to be generated through alternative means, generally by reverse
361 action of ATP synthase and/or by electrogenic exchange of ATP/ADP (43).

362 Asexual blood stage *P. falciparum* rely on glycolysis for ATP generation with little
363 contribution from mitochondrial oxidative phosphorylation (44, 45). Yet the parasite maintains
364 an active mtETC, inhibition of which by antimalarials such as atovaquone results in parasite
365 death. We have previously shown that the critical function of mtETC in blood stage *P.*
366 *falciparum* is to re-oxidize ubiquinol to support mitochondrial DHOD, which is needed for
367 pyrimidine biosynthesis, an essential pathway in the parasites (5). Parasites engineered to
368 bypass mitochondrial DHOD become mtETC independent and resistant to drugs such as
369 atovaquone. We also showed that generation of electropotential across the mitochondrial
370 inner membrane was still required in these mtETC-independent parasites, and that the
371 generation of this potential could be inhibited by proguanil, resulting in parasite death when
372 combined with mtETC inhibitors (5). Since mtDNA in *P. falciparum* encodes just three
373 components of mtETC, we initially reasoned that it should be possible generate rho^0 parasites.
374 However, various attempts failed to generate such parasites (8-10). It is of interest to note that
375 all organisms where rho^0 cells can be generated contain matrix-localized MPP (e.g., yeast,
376 trypanosomes, and mammals), whereas organisms with Complex III associated MPP, such as
377 plants (and *P. falciparum*), cannot be rendered rho^0. Because cytochrome *b* of Complex III is
378 always encoded by mtDNA, maintenance of mtDNA remains essential in these organisms for
379 proper assembly of MPP within Complex III, even when mtETC is made non-essential.
380 A previous study by Espino-Sanchez et al. (46) assessed effects of conditionally knocking
381 down expression of cytochrome c_1, a component of Complex III, in *P. falciparum*. They showed
382 that the parasites lacking this component of Complex III failed to survive but could be rescued
383 by addition of decyl-ubiquinone, consistent with Complex III being the source of ubiquinone to

384 support DHOD. Furthermore, parasites lacking cytochrome c_1 continued to maintain
385 mitochondrial membrane potential, which could be collapsed by treatment with proguanil (46).
386 These results are consistent with prior inferences that Complex III is essential for mtETC activity.
387 In contrast to cytochrome c_1 knockdown, however, we show here that knockdown of MPPα not
388 only results in parasite demise but also a collapsed mitochondrial membrane potential.
389 Parasites with MPPα knockdown cannot be rescued by either the presence of yDHOD or
390 addition of decyl-ubiquinone. Since MPPα is a component of Complex III, our study establishes
391 a secondary role of MPP in addition to maintaining the structure and function of Complex III of
392 mtETC. We posit that this secondary role is to process mitochondrially targeted proteins. In
393 support of this, we observed peptides from multiple mitochondrially targeted proteins in
394 proteomic analyses of MPPα pulldown samples (Figure 5). We suggest that these peptides are
395 generated from proteins transiently associated with Complex III as they are being processed by
396 the MPP subunits.
397
398
399
400
401
402
403
404
405

References

1. Vaidya AB, Lashgari MS, Pologe LG, Morrisey J. Structural features of Plasmodium cytochrome b that may underlie susceptibility to 8-aminoquinolines and hydroxynaphthoquinones. Molecular and Biochemical Parasitology. 1993;58(1):33-42.
2. Fry M, Pudney M. Site of action of the antimalarial hydroxynaphthoquinone, 2-[trans-4-(4'-chlorophenyl) cyclohexyl]-3-hydroxy-1,4-naphthoquinone (566C80). Biochem Pharmacol. 1992;43(7):1545-53.
3. Crofts AR. The Q-cycle - A Personal Perspective. Photosynth Res. 2004;80(1-3):223-43.
4. Mitchell P. The protonmotive Q cycle: A general formulation. FEBS Letters. 1975;59(2):137-9.
5. Painter HJ, Morrisey JM, Mather MW, Vaidya AB. Specific role of mitochondrial electron transport in blood-stage Plasmodium falciparum. Nature. 2007;446(7131):88-91.
6. Vaidya AB, Akella R, Suplick K. Sequences similar to genes for two mitochondrial proteins and portions of ribosomal RNA in tandemly arrayed 6-kilobase-pair DNA of a malarial parasite. Mol Biochem Parasitol. 1989;35(2):97-107.
7. Lamb IM, Okoye IC, Mather MW, Vaidya AB. Unique Properties of Apicomplexan Mitochondria. Annual Review of Microbiology. 2023;77(Volume 77, 2023):541-60.
8. Ke H, Morrisey JM, Ganesan SM, Mather MW, Vaidya AB. Mitochondrial RNA polymerase is an essential enzyme in erythrocytic stages of Plasmodium falciparum. Mol Biochem Parasitol. 2012;185(1):48-51.
9. Ke H, Dass S, Morrisey JM, Mather MW, Vaidya AB. The mitochondrial ribosomal protein L13 is critical for the structural and functional integrity of the mitochondrion in Plasmodium falciparum. J Biol Chem. 2018;293(21):8128-37.
10. Dass S, Mather MW, Morrisey JM, Ling L, Vaidya AB, Ke H. Transcriptional changes in Plasmodium falciparum upon conditional knock down of mitochondrial ribosomal proteins RSM22 and L23. PLOS ONE. 2022;17(10):e0274993.
11. Chacinska A, Koehler CM, Milenkovic D, Lithgow T, Pfanner N. Importing Mitochondrial Proteins: Machineries and Mechanisms. Cell. 2009;138(4):628-44.
12. Wiedemann N, Pfanner N. Mitochondrial Machineries for Protein Import and Assembly. Annual Review of Biochemistry. 2017;86(Volume 86, 2017):685-714.
13. Pollock RA, Hartl FU, Cheng MY, Ostermann J, Horwich A, Neupert W. The processing peptidase of yeast mitochondria: the two co-operating components MPP and PEP are structurally related. Embo j. 1988;7(11):3493-500.
14. Böhni PC, Daum G, Schatz G. Import of proteins into mitochondria. Partial purification of a matrix-located protease involved in cleavage of mitochondrial precursor polypeptides. J Biol Chem. 1983;258(8):4937-43.
15. Taylor AB, Smith BS, Kitada S, Kojima K, Miyaura H, Otwinowski Z, et al. Crystal Structures of Mitochondrial Processing Peptidase Reveal the Mode for Specific Cleavage of Import Signal Sequences. Structure. 2001;9(7):615-25.
16. Dvořáková-Holá K, Matušková A, Kubala M, Otyepka M, Kučera T, Večeř J, et al. Glycine-Rich Loop of Mitochondrial Processing Peptidase α-Subunit Is Responsible for Substrate Recognition by a Mechanism Analogous to Mitochondrial Receptor Tom20. Journal of Molecular Biology. 2010;396(5):1197-210.

449 17. Nagao Y, Kitada S, Kojima K, Toh H, Kuhara S, Ogishima T, et al. Glycine-rich region
450 of mitochondrial processing peptidase alpha-subunit is essential for binding and cleavage of the
451 precursor proteins. J Biol Chem. 2000;275(44):34552-6.
452 18. Iwata S, Lee JW, Okada K, Lee JK, Iwata M, Rasmussen B, et al. Complete structure of
453 the 11-subunit bovine mitochondrial cytochrome bc1 complex. Science. 1998;281(5373):64-71.
454 19. Berry EA, Guergova-Kuras M, Huang L-s, Crofts AR. STRUCTURE AND FUNCTION
455 OF CYTOCHROME bc COMPLEXES. Annual Review of Biochemistry. 2000;69(1):1005-75.
456 20. Brandt U, Yu L, Yu CA, Trumpower BL. The mitochondrial targeting presequence of the
457 Rieske iron-sulfur protein is processed in a single step after insertion into the cytochrome bc1
458 complex in mammals and retained as a subunit in the complex. Journal of Biological Chemistry.
459 1993;268(12):8387-90.
460 21. Yang M, Jensen RE, Yaffe MP, Oppliger W, Schatz G. Import of proteins into yeast
461 mitochondria: the purified matrix processing protease contains two subunits which are encoded
462 by the nuclear MAS1 and MAS2 genes. Embo j. 1988;7(12):3857-62.
463 22. Brumme S, Kruft V, Schmitz UK, Braun HP. New insights into the co-evolution of
464 cytochrome c reductase and the mitochondrial processing peptidase. J Biol Chem.
465 1998;273(21):13143-9.
466 23. Braun HP. The two roles of complex III in plants. Elife. 2021;10.
467 24. Ganesan SM, Morrisey JM, Ke H, Painter HJ, Laroiya K, Phillips MA, et al. Yeast
468 dihydroorotate dehydrogenase as a new selectable marker for Plasmodium falciparum
469 transfection. Mol Biochem Parasitol. 2011;177(1):29-34.
470 25. Concordet JP, Haeussler M. CRISPOR: intuitive guide selection for CRISPR/Cas9
471 genome editing experiments and screens. Nucleic Acids Res. 2018;46(W1):W242-w5.
472 26. Spillman NJ, Beck JR, Ganesan SM, Niles JC, Goldberg DE. The chaperonin TRiC
473 forms an oligomeric complex in the malaria parasite cytosol. Cell Microbiol. 2017;19(6).
474 27. Ganesan SM, Falla A, Goldfless SJ, Nasamu AS, Niles JC. Synthetic RNA-protein
475 modules integrated with native translation mechanisms to control gene expression in malaria
476 parasites. Nat Commun. 2016;7:10727.
477 28. Desjardins RE, Canfield CJ, Haynes JD, Chulay JD. Quantitative assessment of
478 antimalarial activity in vitro by a semiautomated microdilution technique. Antimicrob Agents
479 Chemother. 1979;16(6):710-8.
480 29. Ganesan SM, Morrisey JM, Ke H, Painter HJ, Laroiya K, Phillips MA, et al. Yeast
481 dihydroorotate dehydrogenase as a new selectable marker for Plasmodium falciparum
482 transfection. Mol Biochem Parasitol. 2011 (in press).
483 30. Looareesuwan S, Chulay JD, Canfield CJ, Hutchinson DB. Malarone (atovaquone and
484 proguanil hydrochloride): a review of its clinical development for treatment of malaria. Malarone
485 Clinical Trials Study Group. Am J Trop Med Hyg. 1999;60(4):533-41.
486 31. Srivastava IK, Vaidya AB. A mechanism for the synergistic antimalarial action of
487 atovaquone and proguanil. Antimicrob Agents Chemother. 1999;43(6):1334-9.
488 32. Ke H, Morrisey JM, Ganesan SM, Painter HJ, Mather MW, Vaidya AB. Variation among
489 Plasmodium falciparum strains in their reliance on mitochondrial electron transport chain
490 function. Eukaryot Cell. 2011;10(8):1053-61.
491 33. Lane N, Martin W. The energetics of genome complexity. Nature. 2010;467(7318):929-3
492 34. Martin W, Muller M. The hydrogen hypothesis for the first eukaryote. Nature.
493 1998;392(6671):37-41.

494 35. Stairs CW, Leger MM, Roger AJ. Diversity and origins of anaerobic metabolism in
495 mitochondria and related organelles. Philos Trans R Soc Lond B Biol Sci.
496 2015;370(1678):20140326.
497 36. Tovar J, Leon-Avila G, Sanchez LB, Sutak R, Tachezy J, van der Giezen M, et al.
498 Mitochondrial remnant organelles of Giardia function in iron-sulphur protein maturation. Nature.
499 2003;426(6963):172-6.
500 37. Shiflett AM, Johnson PJ. Mitochondrion-related organelles in eukaryotic protists. Annu
501 Rev Microbiol. 2010;64:409-29.
502 38. Tzagoloff A, Myers AM. Genetics of mitochondrial biogenesis. Annu Rev Biochem.
503 1986;55:249-85.
504 39. King MP, Attardi G. Human cells lacking mtDNA: repopulation with exogenous
505 mitochondria by complementation. Science. 1989;246(4929):500-3.
506 40. Schnaufer A, Clark-Walker GD, Steinberg AG, Stuart K. The F1-ATP synthase complex
507 in bloodstream stage trypanosomes has an unusual and essential function. EMBO J.
508 2005;24(23):4029-40.
509 41. Lill R, Kispal G. Maturation of cellular Fe-S proteins: an essential function of
510 mitochondria. Trends Biochem Sci. 2000;25(8):352-6.
511 42. Stehling O, Elsasser HP, Bruckel B, Muhlenhoff U, Lill R. Iron-sulfur protein maturation
512 in human cells: evidence for a function of frataxin. Hum Mol Genet. 2004;13(23):3007-15.
513 43. Schnaufer A, Domingo GJ, Stuart K. Natural and induced dyskinetoplastic
514 trypanosomatids: how to live without mitochondrial DNA. Int J Parasitol. 2002;32(9):1071-84.
515 44. Sherman IW. Biochemistry of Plasmodium (malarial parasites). Microbiol Rev.
516 1979;43(4):453-95.
517 45. Vaidya AB. Mitochondrial physiology as a target for atovaquone and other antimalarials.
518 In: Sherman IW, editor. Malaria: Parasite biology, pathogenesis, and protection. Washington,
519 DC: ASM Press; 1998. p. 355-68.
520 46. Espino-Sanchez Tanya J, Wienkers H, Marvin Rebecca G, Nalder S-a, García-Guerrero
521 Aldo E, VanNatta Peter E, et al. Direct tests of cytochrome c and c_1 functions in the electron
522 transport chain of malaria parasites. Proceedings of the National Academy of Sciences.
523 2023;120(19):e2301047120.

524

525 **Acknowledgements**

526 We thank Dr. Dale Chaput at University of South Florida Advanced Research Core for Mass

527 Spectrometry for assistance with proteomic analysis. This work was supported by Grant number

528 R01 AI028398 from National Institutes of Health.

529 S1: **Maps of plasmids used for transfections.** Maps of the two gRNA plasmids (A) and (B), and
530 the map for double cross over modification of MPPα locus (C) are shown.

531
532 S2: **MPPα disruption in a second parasite line not expressing yDHOD.**(A) Assessment of
533 growth of MPPα + and MPPα - parasites in Dd2attb parasites. Growth assay was conducted in
534 triplicate by counting 500 parasites via Giemsa stain. (B) Western blot analysis using anti-HA
535 and anti-Aldolase antibodies.
536
537 S3: **Susceptibility of MPPα - parasites to antimalarials remains unchanged.** Parasite growth
538 inhibition assessed by ^{3}H-hypoxanthine incorporation following DSM1, atovaquone, PA21A092
539 treatment. For MPPα - parasites, aTc was removed for 48 h followed by 3H-hypoxanthine
540 addition for 72 hr.
541
542
543
544
545
546

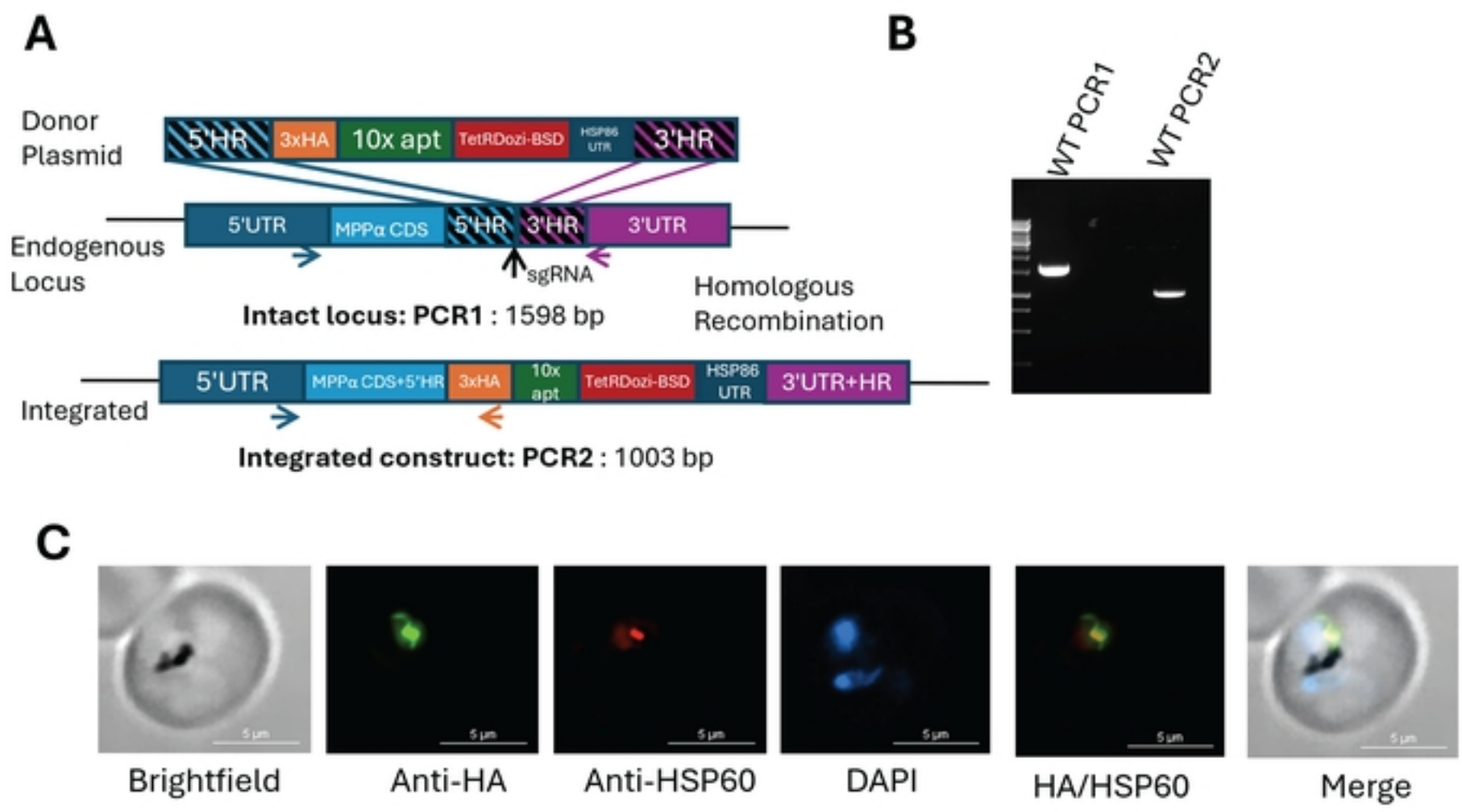
A
Donor Plasmid
5'HR
3xHA
10x apt
TetRDozi-BSD
HSP86 UTR
3'HR
Endogenous Locus
5'UTR
MPPα CDS
5'HR
3'HR
3'UTR
sgRNA
Intact locus: PCR1 : 1598 bp
Homologous Recombination
Integrated
5'UTR
MPPα CDS+5'HR
3xHA
10x apt
TetRDozi-BSD
HSP86 UTR
3'UTR+HR
Integrated construct: PCR2 : 1003 bp
B
WT PCR1
WT PCR2
C
Brightfield
Anti-HA
Anti-HSP60
DAPI
HA/HSP60
Merge

Figure 1

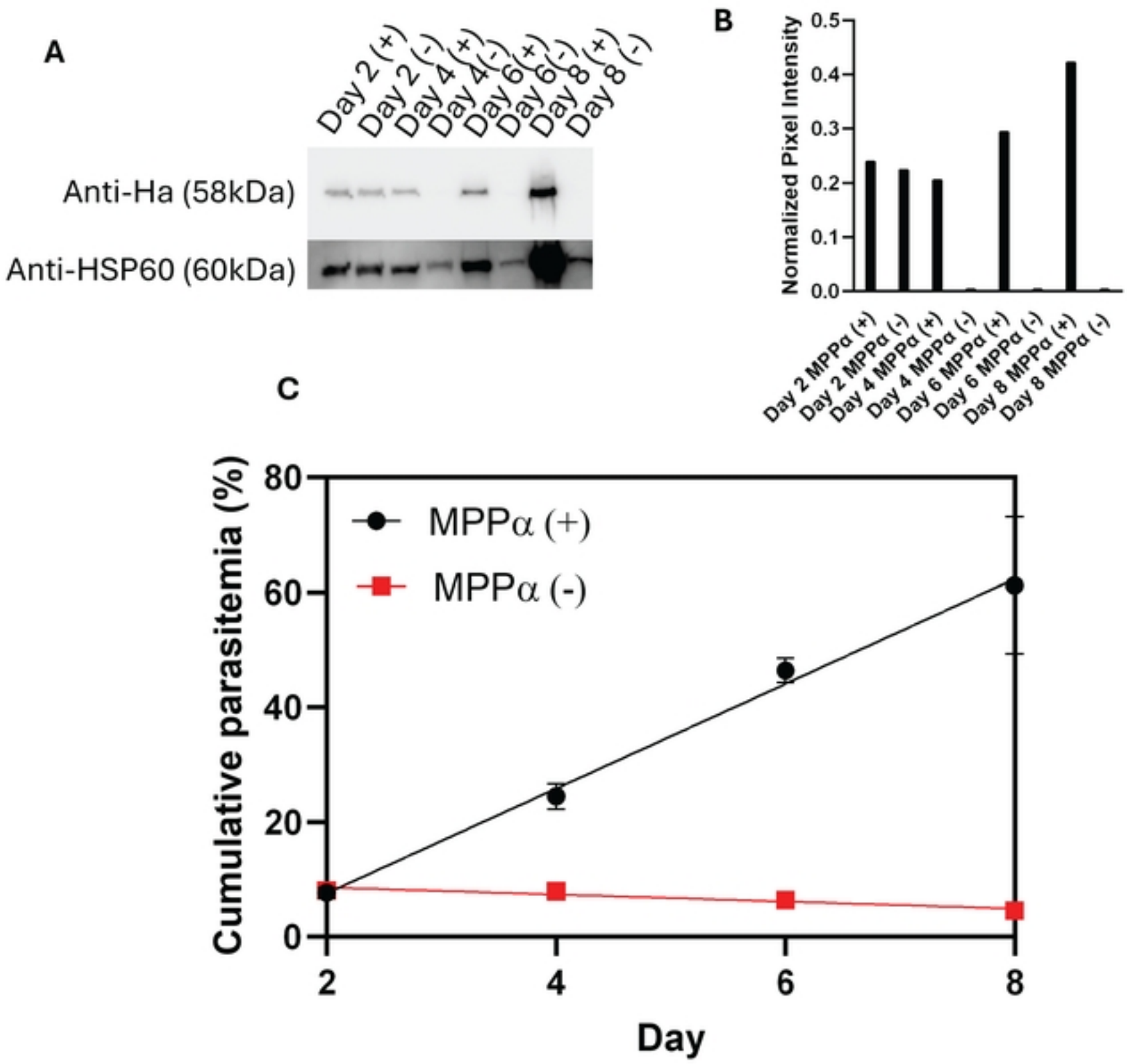
A
Day 2 (+)
Day 2 (-)
Day 4 (+)
Day 4 (-)
Day 6 (+)
Day 6 (-)
Day 8 (+)
Day 8 (-)
Anti-Ha (58kDa)
Anti-HSP60 (60kDa)
B
Normalized Pixel Intensity
0.5
0.4
0.3
0.2
0.1
0.0
Day 2 MPPα (+)
Day 2 MPPα (-)
Day 4 MPPα (+)
Day 4 MPPα (-)
Day 6 MPPα (+)
Day 6 MPPα (-)
Day 8 MPPα (+)
Day 8 MPPα (-)
C
Cumulative parasitemia (%)
80
60
40
20
0
MPPα (+)
MPPα (-)
2
4
6
8
Day

Figure 2

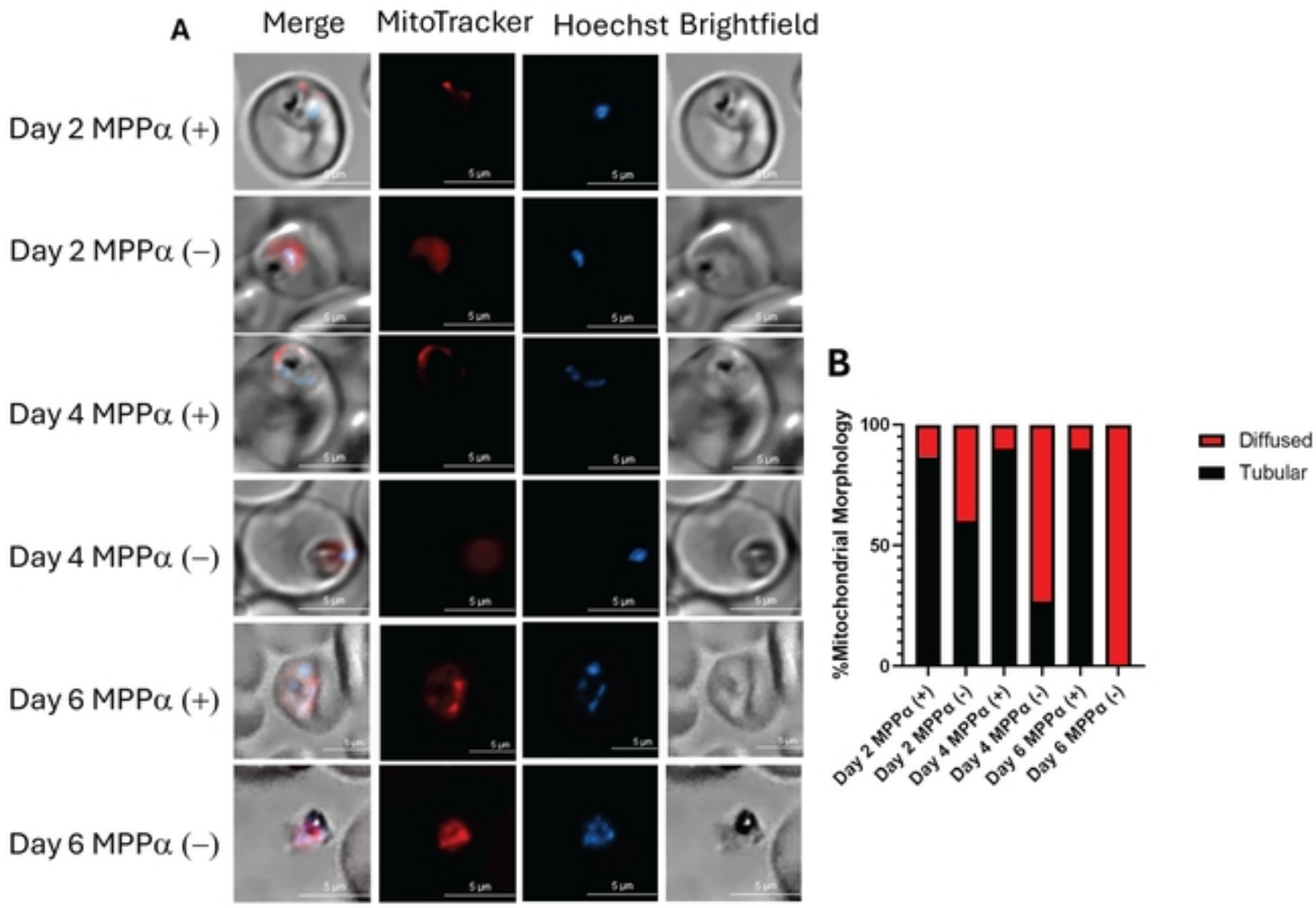
A
Merge
MitoTracker
Hoechst
Brightfield
Day 2 MPPα (+)
Day 2 MPPα (–)
Day 4 MPPα (+)
Day 4 MPPα (–)
Day 6 MPPα (+)
Day 6 MPPα (–)
B
%Mitochondrial Morphology
100
50
0
Diffused
Tubular
Day 2 MPPα (+)
Day 2 MPPα (-)
Day 4 MPPα (+)
Day 4 MPPα (-)
Day 6 MPPα (+)
Day 6 MPPα (-)

Figure 3

A

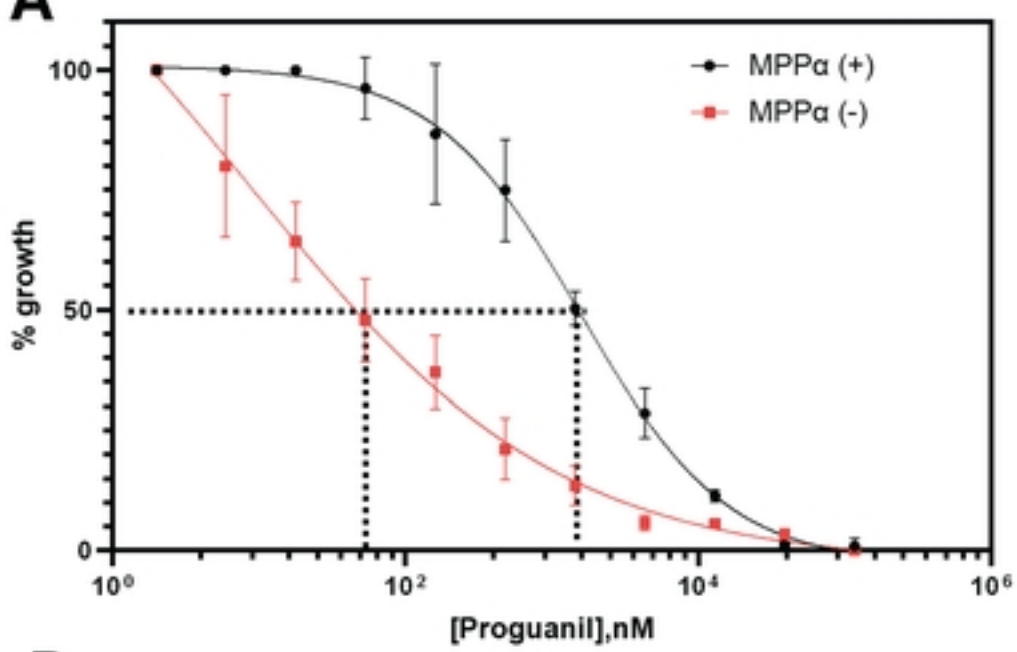

B

Compound	EC50 MPPα (+)	EC50 MPPα (-)
DSM1	> 10,000	> 10,000
Atovaquone	> 10,000	> 10,000
PA21A092	18.9±0.8	21.8±0.6
Proguanil	1585±2.1	84±5.1
Proguanil w/ Decylubiquinone	2785±3.3	107.1±3.6

C

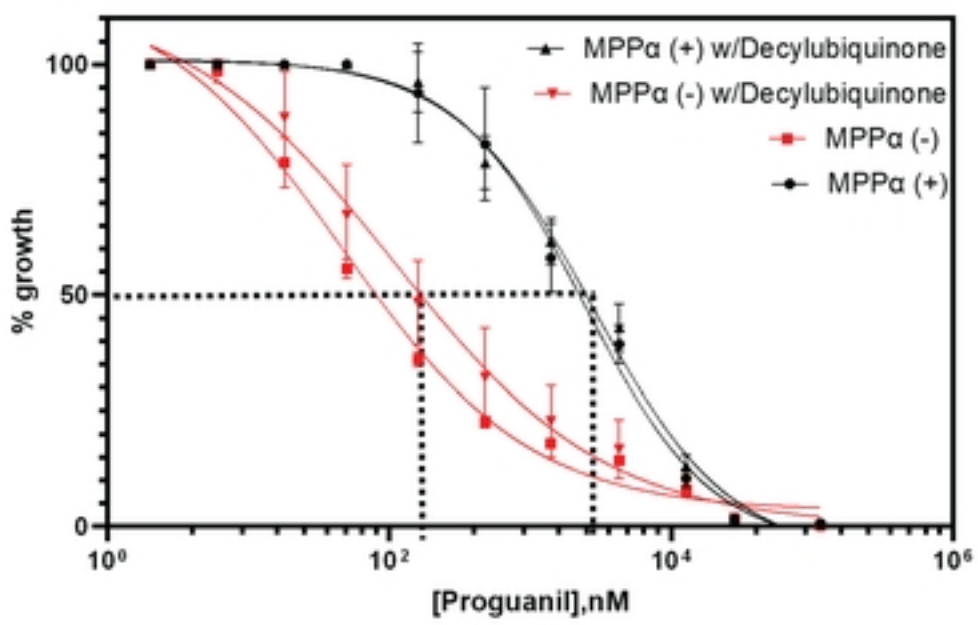

Figure 4

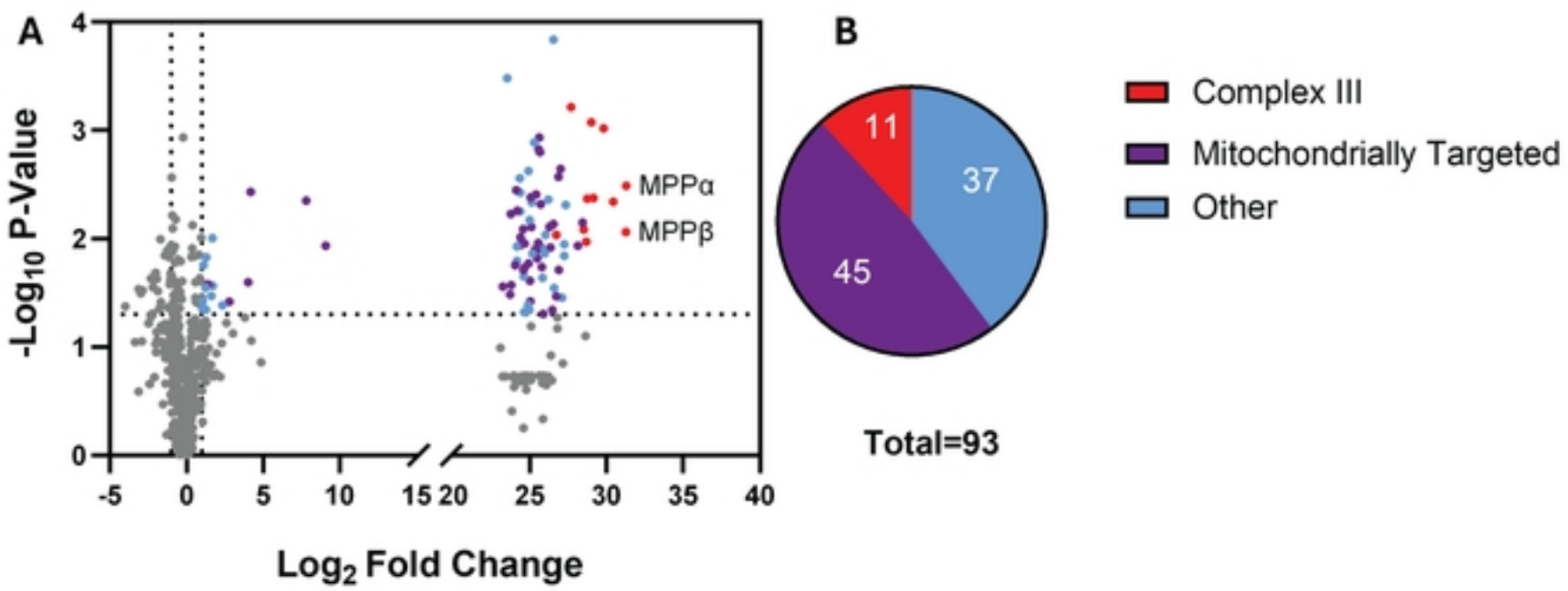
A
B
-Log10 P-Value
Log2 Fold Change
MPPα
MPPβ
Total=93
11
37
45
Complex III
Mitochondrially Targeted
Other

Figure 5